Differences in the regulatory strategies of marine oligotrophs and copiotrophs reflect differences in motility

Stephen E. Noell,[a]* Elizabeth Brennan,[a] Quinn Washburn,[a] Edward W. Davis II,[b] Ferdi L. Hellweger,[c] Stephen J. Giovannoni[a]#

[a]Department of Microbiology, Oregon State University, Corvallis, OR, USA.

[b]Center for Quantitative Life Sciences, Oregon State University, Corvallis, OR, USA.

[c]Water Quality Engineering, Berlin TU, Berlin, Germany.

Address correspondence to Stephen J. Giovannoni: steve.giovannoni@oregonstate.edu

* Present address: Stephen E. Noell, School of Science, University of Waikato, Hamilton, NZ

Running title: Regulation and motility in marine bacterioplankton

Keywords: regulation, copiotroph, oligotroph, chemotaxis, bacterioplankton, alanine, modeling

Abstract

Aquatic bacteria are frequently divided into the lifestyle categories *oligotroph* or *copiotroph*, reflecting adaptations to low and high nutrient availability. In aquatic ecosystems, copiotrophy is associated with chemotaxis and motility, which cells use to find and occupy high-nutrient patches. Oligotrophs have proportionately fewer transcriptional regulatory proteins than copiotrophs, and some have been shown to constitutively express genes involved in the uptake and oxidation of carbon compounds. We hypothesized that the absence of chemotaxis/motility in oligotrophs might prevent them from occupying nutrient patches long enough to benefit from transcriptional regulation. To test this hypothesis, we measured uptake and oxidation of a radiolabeled amino acid, [^{14}C]L-alanine, by a non-motile oligotroph (*Ca.* Pelagibacter st. HTCC7211) and a motile copiotroph (*Alteromonas macleodii* st. HOT1A3). We found that L-alanine catabolism is not transcriptionally regulated in HTCC7211 but is in HOT1A3, initiating within 2.5 – 4 min, as supported by RT-qPCR experiments. L-alanine uptake in HTCC7211 was modulated within 30s by low-amplitude (2-fold) post-translational regulation, a conclusion supported by quantitative analysis with a mechanistic model. By modeling cell trajectories under a range of patch conditions, we predicted that, in most scenarios, non-motile cells spend <2 min in patches, while chemotactic/motile cells occupy patches >4 mins. We conclude that the time necessary to initiate transcriptional regulation prevents non-motile oligotrophs, which drift with currents, from benefiting from transcriptional regulation, but instead have low-amplitude post-translational regulation that can take advantage of their transient passage through a patch.

Importance

Some aquatic oligotrophic bacteria eschew the usual strategy of transcriptionally regulating genes for carbon uptake and metabolism, instead continuously expressing these

systems whether the corresponding carbon compounds are present or not. Often, aquatic oligotrophs lack chemotaxis and motility, while their copiotrophic counterparts use chemotaxis/motility to maximize time spent in patches of high nutrients. We show that diminished transcriptional regulation of carbon catabolism in oligotrophs is due to time limitations: transcriptional regulation takes time, and oligotrophs do not have enough time in nutrient patches for transcriptional regulation to be useful because of their lack of motility. This work enhances our knowledge of the carbon oxidation strategies of marine bacterioplankton and lays the foundation for further theoretical work on this subject.

Introduction

Heterotrophic marine bacteria play a major role in the fate of oceanic organic carbon (Hansell et al., 2009) by respiring as much as 50% of ocean primary productivity (Azam et al., 1983). These organisms employ a variety of life strategies (e.g., *copiotroph* vs. *oligotroph*) to exploit varied opportunities for nutrient acquisition, influencing their success in harvesting dissolved organic matter (DOM) resources. Life strategy categories such as copiotroph and oligotroph are not rigid; rather, microorganisms exist on a continuum within this spectrum. Copiotrophs have been characterized as “feast or famine” bacteria (Koch, 1971) - they are capable of quickly changing growth rate in response to changing nutrient levels, are generally motile (Lauro et al., 2009), and are large in size. Oligotrophs, which are generally non-motile and non-chemotactic in marine systems (Chuckran et al., 2021; Lauro et al., 2009) due to their small cell size (Dusenbery, 1997; Mitchell, 1991), are adapted to live off low nutrient concentrations and thus make only small adjustments in growth rates in response to changes in nutrient concentrations.

A fundamental difference between oligotrophs and copiotrophs that remains relatively unexplored is the reduced transcriptional regulation of carbon uptake and oxidation functions in oligotrophs. Genes associated with regulation are less common in oligotrophs in comparison to copiotrophs (Giovannoni, 2005; Giovannoni et al., 2014; Graham & Tully, 2021; Held et al., 2019; Lambrecht et al., 2020; Lauro et al., 2009). In the oligotrophic SAR11 clade of alphaproteobacteria, many carbon oxidation functions are expressed constitutively (Sun et al., 2016). This is not to say that oligotrophic marine bacteria completely lack transcriptional regulatory mechanisms. In SAR11, several studies have documented low amplitude diel transcriptional changes in a variety of genes, and strong transcriptional responses to iron, sulfur, phosphorous, and nitrogen starvation, which are common causes of environmental stress that have corresponding transcriptional regulators in these cells(Carini et al., 2015; Ottesen et al., 2014; Smith et al., 2010, 2013, 2016). Oligotrophs seem to have evolved reduced transcriptional regulation of carbon uptake and oxidation functions, while retaining post-transcriptional regulatory mechanisms, such as riboswitches, and kinetic regulatory mechanisms (Giovannoni, 2017). In principle, these post-transcriptional mechanisms respond more rapidly to change and require less coding capacity to implement than transcriptional regulation but are not as versatile.

The ocean environment on the microscale is heterogeneous, both in coastal regions and the oligotrophic open ocean (Kostadinov et al., 2009; Pilskaln et al., 2005; Stocker, 2012). There are extreme gradations of nutrient levels in micro-patches in the ocean, such that the exposure of marine bacterioplankton to nutrients is highly variable (Stocker, 2012). Oligotrophs and copiotrophs, due to differences in motility and attachment (Lauro et al., 2009), experience ocean microscales in vastly different ways. Copiotrophs are adapted to maximize their time spent in these nutrient patches, primarily by attaching to phytoplankton and other particulate organic

82 matter or using chemotaxis and motility to identify, move towards, and remain within continuous
83 and ephemeral nutrient patches (Bowen et al., 1993; Lambert et al., 2019; Poindexter, 1981). A
84 growing body of evidence has improved our understanding of the dynamics between nutrient
85 patches and chemotaxis, but questions remain about the regulatory strategies of marine
86 bacterioplankton and the correlation with chemotaxis, which we explore in this project.
87 Oligotrophs inhabit the same patchy environments as copiotrophs (Kostadinov et al., 2009;
88 Stocker, 2012), although they have fewer encounters with patches than chemotactic cells
89 (Blackburn et al., 1998). To explain differences in the regulation of carbon catabolism between
90 oligotrophs and copiotrophs in marine systems, we hypothesized that the lack of chemotaxis and
91 motility in oligotrophs limits their time in patches of nutrients to periods that are too short for
92 transcriptional regulatory systems to initiate and be effective (generally ~3 minutes (Kepes,
93 1963; Pardee & Prestidge, 1961)). The chemotactic ability of copiotrophs in principle allows
94 cells to stay in patches long enough for transcriptional regulatory systems to be fully induced so
95 that cells can reap the benefits of enhanced gene expression. We reasoned that oligotrophs, at the
96 whim of the environment, might rely more on faster-acting and lower amplitude post-
97 transcriptional regulation to take advantage of whatever patches they encounter.
98 To explore this hypothesis, we compared the uptake and oxidation activities of an
99 oligotroph and copiotroph for an organic nutrient common in the ocean, L-alanine (LALA). As
100 our model oligotroph, we chose *Candidatus* Pelagibacter sp. HTCC7211, an open-ocean strain of
101 SAR11 isolated from the Sargasso Sea, since SAR11 cells are the most common group of
102 oligotrophic bacterioplankton in the world (Giovannoni, 2017; Morris et al., 2002). *Pelagibacter*
103 cells have simplified transcription regulatory networks, with only two sigma factors and four
104 two-component systems (Giovannoni, 2005). As our model copiotroph, we chose *Alteromonas*

105 *macleodii* st. HOT1A3, which has a completed genome sequence and was isolated from the open
106 ocean Hawaii Ocean Time series (HOT) site (Fadeev et al., 2016, p. 3). *A. macleodii* is a
107 common marine gammaproteobacterium and has far more complex regulatory systems than
108 SAR11 (Ivars-Martinez et al., 2008). We used LALA as our nutrient because it is widely utilized
109 by marine heterotrophic bacteria via simple and well-characterized metabolic pathways and
110 regulatory systems (Jeong et al., 2015). LALA is primarily metabolized by the reversible enzyme
111 alanine dehydrogenase (ALD) into pyruvate and NH_3, with NAD+ as a cofactor (Berberich et al.,
112 1968); both strains of bacteria used in this study possess a homolog for the *ald* gene.

113 Using this experimental system, we measured uptake and oxidation of [^{14}C]LALA over a
114 series of time points, at a variety of concentrations. We showed that LALA oxidation is under
115 transcriptional regulation in HOT1A3, which we confirmed by reverse transcription quantitative
116 real-time PCR (RT-qPCR) and mechanistic modeling, but is not transcriptionally regulated in
117 HTCC7211. The experimental data and mechanistic model also suggested that HTCC7211 post-
118 translationally regulates LALA uptake. The time necessary for HOT1A3 to initiate oxidation of
119 LALA (2.5 – 4 min) was longer than the simulated residence time of non-motile cells in
120 instantaneous and continuous patches of nutrients under most scenarios (<2 min). We conclude
121 that transcriptional regulation of carbon assimilation pathways would not benefit many
122 oligotrophic marine bacterioplankton because of their lack of motility, and that "always on"
123 uptake and catabolic systems represent a different life history strategy that is advantageous for
124 cells that are not able to direct their motion through the ocean microenvironment.

125 **Results and Discussion**

126 *Exploration of Chemotaxis/Motility Genes in Marine Microbes*

127 In a recent study that divided microbes into oligotroph/copiotroph categories based on
128 maximal growth rates predicted from codon usage patterns (<5h were defined as copiotrophs,
129 ≥5h were defined as oligotrophs), oligotrophs were found to be significantly enriched in motility
130 and signal transduction (including chemotaxis) genes compared to copiotrophs (Weissman et al.,
131 2021). This result is the opposite of what has been previously found (Lauro et al., 2009) and
132 contradicted a main assumption behind our hypothesis. However, this result was based on
133 RefSeq genomes from a variety of habitats. To see if this result held true for marine
134 microorganisms, we repeated the Weissman et al. analysis using metagenome assembled
135 genomes (MAGs) from Tully et al. (Tully et al., 2018). Using the same definition of
136 oligotroph/copiotroph used by Weissman et al., we found that copiotrophs are significantly
137 enriched in genes for signal transduction (including chemotaxis) and non-significantly enriched
138 in genes for motility (Figure S2). This result confirms previous results for marine microbes
139 (Lauro et al., 2009), indicating that the factors affecting the presence of motility and chemotaxis
140 genes in oligotrophs are fundamentally different in marine systems from other systems.

141 *Experimental Observations of L-alanine Uptake and Metabolism*

142 We compared the regulatory strategies of copiotrophs and oligotrophs by measuring the
143 uptake and oxidation of [^{14}C]L-alanine ([^{14}C]LALA) by an oligotroph, *Ca.* Pelagibacter st.
144 HTCC7211, and a copiotroph, *Alteromonas macleodii* st. HOT1A3, to determine the presence of
145 induction in uptake or oxidation of LALA in either strain (Figure 1A-D). The initial
146 concentration of LALA used, 4 μM, is about 100 times higher than the average ambient
147 concentrations of LALA in the open ocean, which are below 100 nM; concentrations of LALA in
148 nutrient patches are generally above 100 nM (Lee & Bada, 1977; X. Lu et al., 2014; Mopper &
149 Lindroth, 1982; Pocklington, 1971). Using collected uptake and oxidation data (depicted in time

150 course plots in Figure 1; experimental data is shown in dots, lines are model results that will be
151 discussed subsequently), rates of uptake, intracellular accumulation, and oxidation were
152 calculated between each time point for each strain by dividing differences in measured values by
153 the difference in time. These calculated rates are depicted in the bar plots in Figure 1. A
154 consistent rate of uptake or oxidation could indicate constitutive expression of the necessary
155 genes and a lack of induction, while an increase in uptake or oxidation rate over time could
156 indicate transcriptional induction. Over the initial 40-min experiment, LALA uptake and
157 oxidation rates in the oligotroph, HTCC7211, remained relatively constant: about 0.5 and 0.3
158 μmol C/g dry weight (DW)/min for uptake and oxidation rates, respectively (Figure 1A-B). In
159 HOT1A3, the rate of LALA oxidation increased throughout the 40-min time course by a log2-
160 fold increase of six as an increasing amount of intracellular LALA was oxidized (Figure 1C-D,
161 Figure S3). The uptake rate of LALA in HOT1A3 remained relatively constant throughout the
162 40-min experiment at an average of 13 μmol C/gDW/min (Figure 1D).

163 Next, we measured the time it took both strains to initiate LALA oxidation at a variety of
164 LALA concentrations. We started with 4 μM LALA, then repeated the experiment, reducing
165 LALA concentrations by a factor of four each time, down to 1 nM. Initiation of oxidation was
166 defined as the first time point when the amount of [^{14}C]LALA oxidized was greater than zero
167 and the standard deviation did not overlap zero (marked by * in Figures 1E-L and 2A-B). In
168 HTCC7211 at 4 μM LALA, oxidation was found to begin between 0.5 and 1 min (Figure 1E).
169 Oxidation initiation times were between 0 and 0.5 min for all concentrations below 4 μM (Figure
170 2A, C). We observed a small but noticeable increase in both uptake and oxidation rates after 0.5
171 min at all concentrations tested above 15.6 nM (Figures 1F, 2A). In HOT1A3 at 4 μM, oxidation
172 initiated at 2 – 2.5 min (Figure 1G-H). This trend continued at concentrations of 1 μM and 250

173 nM, but at concentrations of 62.5 nM and below, oxidation started within the first minute (Figure
174 2B, C). The lone exception was 4 nM, where oxidation initiated around 2 min.

175 We explored this shift in oxidation initiation times in HOT1A3 at concentrations below
176 62.5 nM by repeating the experiment with 62.5 nM out to 40 min to see if the oxidation rate
177 increased at a later time point (Figure 1M-N). However, oxidation and uptake rates stayed
178 constant over the first 10 min at around 1 µmol C/gDW/min for uptake and 0.5 µmol
179 C/gDW/min for oxidation before slowing and ultimately stopping after 20 min as the [^{14}C]LALA
180 was completely removed from the media. The lack of increase in oxidation rate (Figure 1N)
181 indicates that transcriptional induction did not occur in HOT1A3 at 62.5 nM LALA, which is
182 similar to ambient concentrations of LALA in the ocean (Lee & Bada, 1977; X. Lu et al., 2014;
183 Mopper & Lindroth, 1982; Pocklington, 1971). The earlier onset of oxidation at ambient LALA
184 concentrations, defined as 62.5 nM and below, was 1 min, while at patch concentrations (>62.5
185 nM), oxidation initiation started after 2.5 min (Figure 2C). This could indicate that transported
186 LALA is being oxidized primarily by background levels of alanine dehydrogenase at ambient
187 LALA concentrations.

188 To confirm that differences in uptake and oxidation patterns between HTCC7211 and
189 HOT1A3 were due to LALA exposure, we measured uptake and oxidation of 4 µM [^{14}C]LALA
190 using cells pre-conditioned to 4 µM of LALA. In pre-conditioned HTCC7211 cells, uptake and
191 oxidation rates remained constant throughout at around 0.5 and 0.3 µmol C/gDW/min for uptake
192 and oxidation rates, respectively (Figure 1I-J). There was no increase in uptake or oxidation rates
193 from 0.5 to 1 min in pre-conditioned cells (Figure 1I). In pre-conditioned HOT1A3 cells,
194 oxidation initiation occurred at 1 min instead of 2.5 min, and both oxidation and transport rates
195 stayed relatively constant after 1 min at 12 and 7 µmol C/gDW/min for uptake and oxidation

196 rates, respectively (Figure 1K-L). Most strikingly, in HOT1A3 there was a sharp difference in
197 the amount of LALA oxidized between experiments: in pre-conditioned cells at 5 min, 71% of
198 the total LALA taken up had been oxidized, compared to 21% at 5 min in naïve cells, indicating
199 that pre-exposure to LALA in HOT1A3 increased the oxidative capacity of the cells to levels
200 that naïve cells took nearly 40 minutes to reach (Figure 1K-L).

201 We collected transcript data using reverse transcription quantitative real-time PCR (RT-
202 qPCR) to confirm that transcription of the alanine dehydrogenase gene (*ald*, hereafter *ALD* for
203 consistency with our subsequent quantitative model) increased in response to LALA addition in
204 HOT1A3 and not in HTCC7211, and to examine the timing of transcript production (Figure 3).
205 In HOT1A3, in the experimental group that had 4 μM LALA added, transcripts for *ALD*
206 increased immediately compared to the control group, which had the same volume of water
207 added instead (Figure 3A). *ALD* transcription rate was the highest in the first minute after LALA
208 addition, with transcript levels peaking at the 2.5 min time point and staying steady until the last
209 time point collected, 10 min (Figure 3A). In HTCC7211, transcripts were only measured at 0 and
210 5 min as the HTCC7211 phenotype data did not support an increase in HTCC7211 *ALD*
211 transcript levels. No difference was observed between the experimental (4 μM LALA added) and
212 control groups (same volume of water added) at 5 minutes, indicating that *ALD* is constitutively
213 expressed in HTCC7211.

214 Based on these results, we conclude that oxidation of LALA in HOT1A3 is under
215 transcriptional regulation, as indicated by the sharp increase in oxidation rate after 2.5 – 4 min,
216 the continuing increase in the rate of oxidation over time (Figure 1C-D, G-H), the consistent
217 oxidation rate in pre-exposed cells (Figure 1K-L, Figure S3), and the increase in *ALD* transcripts
218 upon LALA addition (Figure 3). This behavior is in accord with genome predictions; the

219 HOT1A3 genome encodes a protein that is homologous to the one responsible for transcriptional
220 regulation of alanine dehydrogenase in *B. subtilis* (Jeong et al., 2015). HTCC7211 does not have
221 transcriptional regulation of LALA metabolism, as indicated by the steady rate of oxidation upon
222 LALA exposure (Figure 1A-B), the similarity in oxidation rates between naïve and pre-exposed
223 cells (Figure 1B, J; Figure S3), the constant expression of *ALD* transcripts (Figure 3B), and the
224 absence of a homolog for the *ALD* regulator in the HTCC7211 genome. We did, however,
225 observe a slight increase in uptake and oxidation rates in HTCC7211 between 0.5 and 1 min at
226 15.6 nM LALA and above, which is most likely due to a regulatory mechanism, since the same
227 increase was not observed in pre-exposed cells (Figure 1I-J, Figure 2, Figure S3).

228 *Quantitative Analysis of Experimental Results*

229 We developed a mechanistic model for regulation of uptake and metabolism of LALA in
230 HTCC7211 and HOT1A3 to further confirm the presence of transcriptional regulation in
231 HOT1A3 for LALA oxidation and test the hypothesis that HTCC7211 used post-translational
232 regulation of LALA uptake. This model is depicted in Figure 4 and the equations and parameters
233 are given in Tables S1-2.

234 In the model, extracellular LALA is transported into cells after diffusion into the
235 periplasmic space either via the alanine:cation symporter (HOT1A3) or the substrate-binding
236 protein (SBP)-dependent ABC amino acid transporter, YhdWXYZ (HTCC7211). Once in the
237 cell, LALA is either incorporated into cellular protein during translation or metabolized to
238 pyruvate by the alanine dehydrogenase enzyme (ALD). In the HTCC7211 model, transcription
239 and translation of the alanine dehydrogenase gene (*ALD*) are continuous due to the absence of
240 transcriptional regulation of *ALD*, while in HOT1A3, transcription of *ALD* starts immediately
241 once LALA is present in the cell (Figure 3A) (Kepes, 1963; Siranosian et al., 1993). As mRNA

242 is produced, translation occurs on ribosomes, incorporating intracellular LALA for 45/377 amino
243 acid residues in ALD. Translated alanine dehydrogenase proteins (ALDN) then undergo enzyme
244 maturation, likely consisting primarily of subunit assembly, since active ALD (ALDM) is
245 comprised of six identical subunits (Porumb et al., 1987).

246 In the HTCC7211 model, the presence of intracellular LALA initiates post-translational
247 regulation that increases the abundance of the periplasmic substrate-binding protein for the
248 LALA transporter, YhdW, by preventing degradation of YhdW. This results in the increased
249 uptake rates after 0.5 min that we observed in HTCC7211 at concentrations above 15.6 nM
250 (Figure 2A, Figure S3). The increased transport rate then results in an increased oxidation rate as
251 more LALA enters the cell. These observed increases in uptake rates are most likely due to a
252 regulatory mechanism, as HTCC7211 cells pre-exposed to LALA exhibited no increase in
253 transport or oxidation rates upon addition of [^{14}C]LALA (Figure 1I-J, Figure S3). This regulation
254 is most likely post-translational, given the fast response time (0.5 – 1 min) exceeds the time
255 needed for translation and enzyme maturation (2 – 4 min) (Kepes, 1963). Additionally, in a
256 previous study, the YhdW protein was found to be more abundant in the absence of nitrogen
257 while *yhdW* mRNA levels were unchanged, indicating that there is at least post-transcriptional
258 regulation of *yhdW* (Smith et al., 2013). In our model, after the initial increase in uptake and
259 oxidation (0.5 – 1 min), uptake and oxidation proceed constantly due to the constitutive
260 expression of *ALD*. There does not appear to be any regulation of LALA uptake in HOT1A3, as
261 there was a similar increase in uptake rate in both naïve and pre-conditioned cells after 10 min
262 (Figure S3). Some increase in both uptake and oxidation rate would be expected, as the cells
263 power up after being starved. The model fit to the data shown in Figure 1 and Figure 2 are
264 depicted by lines.

265 The mechanistic models supported the different interpretations of regulation of LALA
266 uptake and metabolism in the two strains. Regulation was turned off by changing parameters,
267 then the model was re-optimized to fit the data with those restrictions (see Methods for full
268 description). The alternate parameters without regulation are given in Table S2. In both cases,
269 the model fit the data better with regulation included, as the normalized sum of error squared
270 (SES) values were lower with regulation (2.53 and 2.24 for HTCC7211 and HOT1A3,
271 respectively) than without (3.78 and 2.78 for HTCC7211 and HOT1A3, respectively).

272 The nature of the post-translational regulation implicated in HTCC7211 LALA uptake
273 cannot be determined from the data at hand, but could be either due to a post-translational
274 modification (PTM) (Macek et al., 2019) or a change in translational efficiency (Al-Bassam et
275 al., 2018; R. C. Taylor et al., 2013). Given the previously observed uncoupling between *yhdW*
276 mRNA and YhdW protein abundances in SAR11 under nitrogen limitation (Smith et al., 2013),
277 it is likely that there is a mechanism increasing the abundance of the YhdW protein in response
278 to LALA. There are two PTMs known to be involved in modulating the stability of proteins: N^{α}-
279 acetylation, which requires acetyltransferases (Liang et al., 2011), and pupylation (Striebel et al.,
280 2014). N^{α}-acetylation is the more likely possibility in HTCC7211, given that pupylation has
281 previously only been observed in *Mycobacterium* and there are multiple uncharacterized
282 acetyltransferases in the HTCC7211 genome. Protein turnover rates on the order of minutes have
283 been previously observed in other bacteria, making the acetylation mechanism plausible (Maier
284 et al., 2011). Another possibility is that the cells use a PTM to increase the binding affinity of the
285 SBP to LALA.

286 The data and mechanistic model also suggested that transcriptional regulation of *ALD* in
287 HOT1A3 is not induced at ambient levels of LALA, since the model predicts that ALDM levels

288 do not appreciably increase in cells exposed to 62.5 nM LALA compared to cells exposed to 4
289 μM LALA (Figure S4). The model predicts that the amount of LALA entering cells is not large
290 enough to induce transcription of *ALD*. In the environment, HOT1A3 cells would not benefit
291 from induction at ambient LALA concentrations, since they would not be bringing in enough
292 LALA to support cellular growth. The oxidation that was observed at 62.5 nM LALA and below
293 is also predicted by the model to be due to background ALDM levels in the cell. Background
294 activities of ALDM were measured in *Bacillus licheniformis* to be between 0.02 – 0.04 IU/mg of
295 protein (McCowen & Phibbs, 1974). If this background activity were occurring in HOT1A3, we
296 would expect to observe an oxidation rate of 2.84 – 10.33 μmoles C/gDW/min. The total rate of
297 oxidation observed at 62.5 nM was 0.4 μmoles C/gDW/min, well below this range, implying that
298 this is a reasonable explanation for the results. Another possible explanation is that the oxidation
299 observed at 62.5 nM LALA is due to a different pathway of LALA metabolism that is not
300 inducible, which is plausible because there are two pathways that could potentially metabolize
301 LALA in HOT1A3, via an alanine racemase or an alanine-glyoxylate transaminase. Follow-up
302 transcriptome and proteome studies would be needed to evaluate if these pathways play a major
303 role in LALA oxidation and if they are under transcriptional regulation.

304 The 2.5 – 4 min lag between the addition of LALA and the initiation of oxidation in
305 HOT1A3 is primarily due to translation and ALD protein maturation. In an exploration of
306 inducible enzymes in *E. coli*, a similar lag time of 3 min was observed, with transport and
307 transcription occurring quickly (< 0.5 min) and translation and enzyme maturation splitting the
308 remaining lag time (Kepes, 1963; Pardee & Prestidge, 1961). Similarly, previous studies of ALD
309 found that transcription of *ALD* initiated immediately and peaked around 1.5 min (Freese &
310 Oosterwyk, 1963; Siranosian et al., 1993). Our RT-qPCR data showed *ALD* transcription started

311 immediately in HOT1A3; transcript levels peaked at 2.5 min, similar to our mechanistic model
312 prediction of a 4 min peak (Figure S4B). However, our mechanistic model predicted a sharp
313 decrease in *ALD* transcripts after the peak, which was not observed in our RT-qPCR data. One
314 potential implication is that mature ALD enzymes are less stable than predicted in our
315 mechanistic model.

316 *Regulation and Motility*

317 We hypothesized that the lack of transcriptional regulation in oligotrophs is related to
318 non-motility, which prevents oligotrophic cells from inhabiting patches of nutrients long enough
319 for transcriptionally regulated systems to turn on. It has been observed before that oligotrophs
320 are primarily non-motile, while copiotrophs are generally motile (Lauro et al., 2009), an
321 observation that is also true in our experimental system. We expected that this difference in
322 motility would also translate into a difference in exposure to nutrients, which would have an
323 impact on the ability of transcriptional regulatory systems to function. To further explore this
324 relationship between motility and regulatory strategy, we predicted residence times of motile
325 (copiotrophic) and non-motile (oligotrophic) bacteria as individuals in an environment with
326 either a continuous or instantaneous nutrient source. A continuous source of nutrients would be
327 akin to proximity to a leaking phytoplankton cell or a detritus particle, whereas an instantaneous
328 patch would be similar to a bursting cell. Non-motile cells drifted randomly throughout the
329 environment, simulating diffusion, while motile cells moved upgradient using a run-reverse-flick
330 chemotaxis, which was implemented based on (Son et al., 2016). We present results for a range
331 of initial distances of the bacteria to the source (Near, Middle, Far) in Figure 5B-C. A
332 representative model run with a continuous source and cells placed at the Middle distance from
333 the source is shown in Figure 5A.

For the scenarios where cells are placed near the source, the cells either start in the patch (continuous source) or are quickly engulfed by the diffusing concentration (instantaneous source) (Figure 5B-C). For the instantaneous source, a few of the motile cells wander away early and do not find their way back to the patch. Both cell types remain in the patch for relatively long times (>10 min). For the non-motile cells, this can be attributed to their lower effective diffusivity. The motile cells have a higher effective diffusivity, but that is successfully counteracted by the chemotaxis. However, the near-source scenario is unlikely and it is much more probable that the cells are further away from the nutrient source (e.g., the probability increases with the square of the distance) (Hulburt, 1970; Siegel, 1998). For the middle scenario, a larger fraction of the motile cells reach the patch than non-motile cells, which is probably the main benefit of chemotaxis. However, chemotaxis also affects the patch residence time, which is important for regulation. Specifically, the model predicts that, of the cells that reach the patch, the motile cells spend more time in the patch (>6 min) than the non-motile cells (<2 min). For the far distance scenario, the number of cells that reach the patch and the patch residence times decrease further.

The results of our simulation depend on the choice of parameters (e.g., the size of the continuous nutrient source, see Figure S6) and further modeling work will be required to fully characterize the distribution of patch residence times. However, across the tested sets of parameter values, the motile cell always (except the instantaneous far scenario, Figure 5C) stays in the patch long enough for cells to be fully induced and begin acquiring energy from LALA (oxidation initiation), which we measured at 2.5 – 4 min in HOT1A3. In most scenarios, the non-motile cell does not occupy the nutrient patch for more than 2 min (except the near scenarios, Figure 5B-C, and the high source size scenario, Figure S6).

The low occupancy time predicted from our model for non-motile cells supports our hypothesis that non-motile oligotrophs do not occupy nutrient patches long enough for transcriptional regulation to be viable. The lack of transcriptional regulation in non-motile oligotrophs like SAR11 results in them not missing the opportunities they would have missed if they relied on transcriptional regulation. The drawback is that the magnitude of their regulatory response is much lower than copiotrophs (HTCC7211 cells had a log2-fold increase of 1.5 in uptake rate after 30 s, compared to a 6-fold increase in oxidation rate in HOT1A3 over 40 min (Figure S3)).

In previous studies, clusters of chemotactic bacteria around nutrient patches were found to reach peak density within 5 min; however, time spent in the patch of nutrients by individual cells was not measured (Blackburn et al., 1998; Luchsinger et al., 1999; Seymour et al., 2009; Stocker et al., 2008). On the other hand, in lab settings with limited shear, the mean residence time of individual chemotactic cells in a 0.2 mM patch of tryptone was 35 min, with residence time increasing with higher tryptone concentrations (Yawata et al., 2020). Instantaneous nutrient patches have been measured to be either exhausted by microbial uptake or dispersed by shear within 10 min (Blackburn et al., 1998), but sinking particles could provide opportunities for chemotactic cells to stay at high nutrient concentrations for longer time scales. Previous studies have shown that non-motile cells have fewer encounters with nutrients, with non-motile cells encountering half (Blackburn et al., 1998), one-fourth (Stocker et al., 2008), or one-fifth (Brumley et al., 2019) the amount of nutrients in a patch as motile cells, but the relationships between motility and transcriptional regulation were not explored in these studies.

The lack of motility in oligotrophs like SAR11 may be linked to small cell size, since cells the size of SAR11 would not be able to overcome Brownian effects, making chemotaxis

379 impossible (Mitchell, 1991). However, some oligotrophic bacteria, for example the SAR92
380 clade, are motile. SAR92 was reported to have minimal transcriptional regulation (Cottrell &
381 Kirchman, 2016), but those experiments reported variation in transcription between cells in
382 exponential growth phase and cells entering stationary growth phase, rather than responses to the
383 availability of carbon resources. In *Pelagibacter*, a similarly small level of transcriptional
384 (Cottrell & Kirchman, 2016) and proteomic (Sowell et al., 2008) changes were observed upon
385 entering stationary phase, which is attributable to the lack of σ^S, the stationary phase sigma factor
386 found in many proteobacteria (Sowell et al., 2008). If the relationship between motility and
387 regulation of carbon assimilation pathways that we describe is generally true, then it would be
388 expected that a motile oligotroph like SAR92 would not be deficient in regulation of carbon
389 assimilation pathways, but would lack σ^S, like *Pelagibacter*.

390 **Conclusion**

391 With experiments and models, we demonstrate that, as "feast and famine" bacteria,
392 copiotrophs can employ motility to stay in patches of nutrients long enough to sense compounds
393 and increase metabolic activity using transcriptionally regulated systems. Between patches, they
394 leave many catabolic systems turned off, minimizing the cost of synthesizing un-needed proteins.
395 Oligotrophs, as "fast and famine" bacteria, are at the whim of their environment and experience
396 random encounters with nutrient patches they briefly exploit before drifting out of the patch. We
397 show that these cells constitutively express genes involved in carbon uptake and metabolism, not
398 missing fluctuating opportunities to transport and metabolize the nutrients they need to survive,
399 but likely failing to make the most of unusual episodes of high nutrient concentrations.
400 Notwithstanding their limited transcriptional responses, oligotrophs appear to have post-
401 transcriptional, and in this study, post-translational, controls on metabolism that enable them to

402 respond more rapidly but with much smaller amplitude to fleeting opportunities. Post-
403 transcriptional regulatory systems have been observed before in oligotrophs (Cottrell &
404 Kirchman, 2016; Held et al., 2019; Lankiewicz et al., 2016; Meyer et al., 2009; Ottesen et al.,
405 2014; Scanlan et al., 2009; Tripp et al., 2009), as would be expected in cells that are adapted to a
406 life of constant nutrient limitation (Button, 2004). Our findings add to conceptual models by
407 linking the non-motile, small genome, solitary cell phenotype often observed in planktonic
408 oligotrophs to a strategy of continuously expressing genes for carbon oxidation pathways.

409 **Materials and Methods**

410 *Bioinformatics*

411 To compare the prevalence of motility and chemotaxis genes in oligotrophs and
412 copiotrophs, metagenome assembled genomes (MAGs) from the Tully et al. marine data set
413 (Tully et al., 2018) were downloaded from the NCBI assembly database using get_assemblies v
414 0.8.6 using the settings 'assembly_ids --function genomes -o fna --force'
415 (https://github.com/davised/get_assemblies). One genome was randomly picked from each
416 genus, for a total of 250 genomes (for a list of genomes, see Table S4). Proteins were annotated
417 using bakta v 1.4.0 with default parameters (Schwengers et al., 2021). The commandline rpsblast
418 v 2.13.0 was used to search annotated protein sequences as queries against the latest (date 2021-
419 02-22) COG database subset of the Cdd (Camacho et al., 2009; S. Lu et al., 2020). Tabular
420 output from the rpsblast was converted from Cdd ID to COG ID using the data from the
421 COG2020 release from NCBI (Galperin et al., 2021). For each protein, COG functions were
422 assigned using a two-tier filtering approach. The assigned bitscore cutoffs for each COG in the
423 2020 release were used as a first step filter, where COG hits below the bitscore cutoff were
424 discarded. Then, of the COG hits remaining, the COG with the highest bitscore was assigned to

425 each protein. COG Categories were assigned based on the COG2020 annotations for each COG.
426 Genomes were then categorized as copiotrophs or oligotrophs based on their predicted maximal
427 growth rates, which were taken from (Weissman et al., 2021). The proportion of genes within
428 each category was calculated for each genome; significant enrichment was tested using Mann–
429 Whitney tests with a Benjamini–Hochberg correction (α=0.05).

430 *Growth and Washing of Cultures*

431 *Candidatus* Pelagibacter sp. HTCC7211 and *Alteromonas macleodii* st. HOT1A3 were
432 both originally isolated from open ocean, oligotrophic sites (Sargasso Sea and HOT station
433 ALOHA, respectively) (Sher et al., 2011; Stingl et al., 2007). Cultures were grown on artificial
434 seawater (ASW) (Carini et al., 2013). SAR11 cells were grown in ASW amended with 100 µM
435 pyruvate, 50 µM glycine, 10 µM methionine, and SAR11-specific vitamins (Carini et al., 2013,
436 2014). HOT1A3 cultures were grown in ASW amended with 1 mM acetate, lactate, pyruvate, 0.5
437 mM glycerol, and a general vitamin mix (Fadeev et al., 2016). For experiments where cultures
438 were pre-exposed to LALA prior to washing, 4 µM LALA was added to the cultures two
439 generations before harvesting. For HTCC7211, with an average doubling time of 1.4 days,
440 LALA was added 3 days prior to harvesting, while LALA was added 3 hours prior to harvesting
441 HOT1A3 cultures, as their average doubling time was 1.5 h.

442 Cultures were grown at 25˚C in a shaking incubator at 85 RPM in 12 h light/dark to late
443 exponential phase before harvesting. Cells were harvested to concentrate cells and remove
444 extracellular organics using centrifugation on a Beckman J2-21 Centrifuge at 10˚C at 30,000 g
445 for either 90 min (HTCC7211) or 30 min (HOT1A3), followed by washing in ASW with no
446 added organics in a Beckman-Coulter Ultracentrifuge at 10˚C at either 48,000 g for 60 minutes
447 (HTCC7211) or 28,000 g for 20 min (Noell & Giovannoni, 2019). Supernatant was removed and

448 the cells were re-suspended in ASW with no added organics. The centrifugation protocol used
449 here matches that used previously in our lab, where cell viability was tested using flow
450 cytometry and growth experiments (Giovannoni et al., 2019; Noell et al., 2021; Noell &
451 Giovannoni, 2019). In previous tests, no changes in forward and side scatter or DNA
452 fluorescence peaks were observed using flow cytometry in SAR11 cells that underwent these
453 treatments. SAR11 cells that underwent these treatments grew normally when put back into
454 growth media (see the positive control cultures in the growth experiments in (Noell &
455 Giovannoni, 2019)).

456 *Uptake Experiments*

457 Washed cultures were pooled to the desired volume at a cell density between 2 – 8 E7
458 cells/mL and cell counts taken, as previously described (Carini et al., 2013). Pooled cultures
459 were divided into appropriate volumes in individual BSA-coated septum vials and sealed with
460 PTFE-faced butyl septa (Millipore-Sigma, 27201) (Halsey et al., 2012). A portion of the cultures
461 were heated at 50˚C for 1 h to make the killed-cell controls. Metabolic activity of cultures was
462 slowed by chilling at 4˚C in the dark until counting finished, 1 h, to induce a partial starvation
463 state similar to that experienced by most cells in the ocean (Moriarty & Bell, 1993; Morita,
464 1982). Cultures were kept in the dark throughout to remove any possibility of cells gaining
465 energy from rhodopsins (Steindler et al., 2011). Cultures were warmed to room temperature
466 using a heater prior to the start of uptake experiments. As above, these steps follow previously
467 used protocols and the impact of cooling/heating on cell viability was minimal (Noell &
468 Giovannoni, 2019). Reagents were added to cultures via injection with syringe and needle
469 through the stoppers. [^{14}C]L-alanine (American Radiolabeled Chemicals, ARC 0231, [1-14C])
470 was added to the cultures at the desired final concentration. Cultures were then incubated for the

471 needed time in a dark water bath at 25˚C. The reaction was stopped by the addition of either 10
472 mM sodium azide (for the intracellular fraction) or 0.05 N NaOH, 2.5 mM Na_2CO_3, and 50 mM
473 $BaCl_2$ (for the total fraction: intracellular + oxidation to $^{14}CO_2$). Intracellular fraction cultures
474 were then placed on ice and filtered within 2 h, while total fraction cultures were placed at 4˚C
475 overnight before filtering (Halsey et al., 2012). Cultures were filtered on 0.1 or 0.2 µm PTFE
476 Omnipore Membrane filters (HTCC7211 and HOT1A3, respectively), washed three times with 3
477 mL of un-amended ASW to remove extracellular ^{14}C label, and transferred to scintillation vials
478 with scintillation fluid (Ultima Gold XR, Perkin Elmer) and left overnight prior to counting.
479 Triplicate cultures were used for each time point for each fraction, for a total of six
480 cultures for each time point. Raw counts from a blank filter were subtracted from each sample.
481 To calculate the $^{14}CO_2$ produced (oxidized fraction), the ^{14}C signal in the intracellular fraction
482 was subtracted from the total fraction. Average ^{14}C signal in the time-zero time points for each
483 fraction was subtracted from all other time points in that fraction to account for variability
484 between the two methods used, as it takes longer for the azide reagent to be added than the
485 multiple reagents required for the $BaCl_2$ method. Total uptake rates were calculated by dividing
486 differences in total fraction values by difference in the time between those points. The total
487 fraction was used for this as it represents the total amount of [^{14}C]LALA that fluxed into the cell.
488 Oxidation rates were calculated in the same way using the oxidation values for time points.
489 Figures were plotted using the ggplot2 package in the R software environment (R Core Team,
490 n.d.; Wickham, 2016).

491 *RNA extraction and RT-qPCR*

492 RNA was extracted from HOT1A3 and HTCC7211 cells to measure transcript changes in
493 *ALD* in response to LALA addition. High cell density cultures of HOT1A3 and HTCC7211 were

494 prepared as described above, final volume of 10 mL (final cell density of ~1E10 cells/mL). To
495 the experimental cultures, LALA was added at 4 µM, while an equal volume of sterile water was
496 added to negative control cultures. Cultures were incubated as described above for various times,
497 then placed on ice to stop cell activity. Cells were then pelleted via centrifugation, maintaining
498 0˚C temperature throughout. Pellets were re-suspended in RNAlater solution (Life Technologies,
499 AM7020) at room temperature for 15 min, pelleted again via ultracentrifugation, then flash
500 frozen in liquid nitrogen following supernatant removal and stored at -80˚C until RNA extraction
501 was performed. For HOT1A3, biological duplicates were performed for each time point and
502 treatment group, which were each split into technical duplicates prior to RNA extraction, for a
503 total of 4 replicates. For HTCC7211, biological quadruplicates were performed for the two time
504 points.

505 RNA extraction was performed using an RNeasy min-elute cleanup kit (Qiagen, 74204)
506 with an on-column DNase treatment (Qiagen, 79254) and a 5 minute incubation with buffer
507 RW1 to enhance genomic DNA (gDNA) removal per the manufacturer's instructions. Samples
508 were eluted in 20 µL of RNase-free water and stored at -80˚C until further analysis. Remaining
509 contaminating gDNA was removed using the Thermo Fisher Turbo DNA-free kit (Life
510 Technologies, AM1907), following the manufacturer's recommendation of carrying out two
511 separate incubations with half the total DNase (30 min each) on each sample. Total RNA was
512 quantified via Qubit fluorometer (Thermo Fisher) and RNA quality assessed using the
513 BioAnalyzer 2100 (Agilent) RNA Nano Chip at the Center for Genome Research and
514 Biocomputing Core Facilities at Oregon State University. All samples had no signs of RNA
515 degradation and had rRNA ratios between 1.5 and 2.

516 For reverse transcription quantitative real-time PCR (RT-qPCR), the procedure used was
517 similar to (Schuster, 2011). 300 ng of RNA from each sample was reverse transcribed into
518 cDNA using the Qiagen QuantiTect RT kit (Qiagen, 205311) following the kit instructions, final
519 volume of 20 µL. Negative controls with no template RNA added and with no reverse
520 transcriptase added were included to check for contaminating gDNA or procedural
521 contamination, which was checked with PCR and gels; no contamination was observed (data not
522 shown). Primers were designed for the *ala* gene and two endogenous control genes (*recA* and
523 *rpoD*) with T_m values close to 65˚C using the Geneious Primer Design tool, which screens for
524 off-target sites. Primers were ordered from Integrated DNA Technologies with standard
525 desalting. Primer sequences are given in Table S5. Primers were validated on DNA from the
526 organism of choice (*A. macleodii* st. HOT1A3 or *Cand.* P. st. HTCC7211) using PCR; no off-
527 target amplification was observed, with a single, strong band for each primer in each strain (data
528 not shown). qPCR was performed using the Qiagen QuantiTect SYBR Green PCR kit (Qiagen,
529 204143) on an Applied Biosystems 7500 Real-Time PCR System, with a final reaction volume
530 of 25 µL; all reagents followed the manufacturer's recommendations. A primer concentration of
531 0.2 µM was used and 1 µL of 1:10 diluted cDNA sample was added. Optical 96-well reaction
532 plates (Life Technologies, 4346906) were sealed with clear adhesive film (Life Technologies,
533 4306311) and centrifuged briefly prior to placing into instrument. Instrumental qPCR parameters
534 are as follows: initial activation (95˚C, 15 min), 40X cycles of denaturation (94˚C, 15 s),
535 annealing (60 or 55˚C for HOT1A3 and HTCC7211, respectively, for 30s), and extension (72˚C,
536 30 s), followed by a standard melt curve analysis. No-template controls were included to assess
537 contamination; in all controls, either no amplification or C_q values above 37 were observed. Melt
538 curves all showed a single peak for each primer (Figure S1A-E). Each experimental sample was

539 measured in duplicate for qPCR. Primer efficiencies were measured for each HOT1A3 primer
540 using a 5X 1:10 dilution series (in duplicate) of cDNA samples and were all above 93%.
541 Endogenous control genes were tested for constant expression across all time points and
542 experimental groups (Figure S1F-G). Data analysis was conducted in Microsoft Excel using the
543 method described by (Vandesompele et al., 2002) for normalizing gene expression to multiple
544 endogenous control genes. The average value of the control group time zero replicates was used
545 as the calibrator for calculating ΔC_T values. Data was extracted from runs using the 7500 FAST
546 System software (v 2.0.6).

547 *Mechanistic Model*

548 A mechanistic model of LALA uptake and metabolism, as well as regulation of those
549 processes, was developed for the two strains of bacteria used in this study. A list of the equations
550 used can be found in Table S1. The model was coded into Excel and parameterized using values
551 from literature and from experiments (Table S2). The parameters were optimized to fit all
552 experimental data using the SOLVER add-in in Excel by setting it to minimize the summated,
553 normalized sum of error squared value (SES) from the fit of the model to all experimental data.
554 To calculate the SES, the experimental and model values for each experiment were first
555 converted to molC/L, then normalized using the mean of all experimental values from that
556 experiment. The SES was calculated using these normalized values, then divided by the number
557 of data points for that experiment, so that experiments with larger number of data points would
558 not have oversized influence on the optimization. SOLVER was run with the following settings:
559 Evolutionary solving method, convergence of 1E-9 (to allow for optimizing low K_m values),
560 mutation rate of 0.075, population size of 500, maximum time without improvement of 240 s,
561 with bounds on variables and automatic scaling. Multiple runs of SOLVER were required, using

562 different starting points, to achieve an optimal fit of the model to the data. The starting state for
563 the model for the pre-induced experiments was set to be equal to the final state from the model
564 fit to the 4 μM 40-min experiment.

565 We tested for the presence of regulation in HTCC7211 and HOT1A3 on LALA uptake
566 and *ALD* transcription, respectively. In HTCC7211, $K_{a,tran,LALA}$ was set very low (1E-20) and
567 $n_{a,tran,LALA}$ was set high (15), so that the activation term for uptake equaled one. Similarly, in
568 HOT1A3, $K_{a,rpom,LALA}$ and $n_{a,rpom,LALA}$ were also set so that the activation term for transcription of
569 *ALD* equaled one, and cellular levels of *ALD* transcript, naïve protein, and mature enzyme
570 ($Q_{ALDT(2)}$, $Q_{ALDN(2)}$, and $Q_{ALDM(2)}$, respectively) were set to be equal to the maximum values from
571 the model fit to the 4 μM 40-min experiment, to reflect a state of constitutive expression.

572 *Estimation of Patch Residence Time*

573 The purpose of the patch residence model is to estimate the residence time of motile and
574 non-motile bacteria in instantaneous (i.e. a lysing phytoplankton cell) and continuous (i.e.
575 exudation from a live phytoplankton cell) DOM patches (see Supplemental Methods for full
576 description). Three-dimensional and time-variable (for the instantaneous source) substrate
577 concentrations are computed. Trajectories of motile and non-motile bacteria are computed and
578 their patch residence time is computed based on a threshold concentration (C_{in}, molC/m^3). Motile
579 and non-motile bacteria are modeled as individual agents. They diffuse using a random walk
580 (Hellweger & Bucci, 2009) based on a diffusion coefficient (D, m^2/s). In addition, motile
581 bacteria move with a run-reverse-flick mechanism, which was implemented based on (Son et al.,
582 2016). A benchmark test of our model against experimental results from that paper is shown in
583 Figure S5B and a benchmark test of the run & tumble component of our model against the model
584 in (Jackson, 1987) is shown in Figure S5A.

Model parameters were chosen to represent a realistic scenario (Table S3, Supplemental Methods). Diffusivities of motile and non-motile bacteria were estimated from observed cell sizes for copiotrophs and oligotrophs (Table S3, Supplemental Methods). The concentration marking the boundary between inside and outside of the patch (C_{in}, used for Figure 5B-C) was taken at 10 µmolC/L (10,000 nmolC/L), a value considerably above background DOM concentration for the open ocean (0.1 – 50 nmolC/L, (J. R. Taylor & Stocker, 2012)). The instantaneous release mass (M) was taken to be large enough so that the patch exists (max. $C > C_{in}$) longer than the time it would take cells to transcriptionally upregulate their transport system.

Data Availability

All experimental data (uptake and qPCR data) and models (mechanistic biochemical model) as well as the associated scripts for analysis and plotting the figures are freely available on Github (https://github.com/stenoell/Noell-oligo-copio-regulatory-strategies). The patch model is available on a separate Github page (https://github.com/fhellweger).

Acknowledgments

The authors thank Dr. Daniel Sher at the University of Haifa for providing the *Alteromonas macleodii* st. HOT1A3 strain for this project. This work was funded by the National Science Foundation grant IOS-1838445.

References

Al-Bassam, M. M., Kim, J.-N., Zaramela, L. S., Kellman, B. P., Zuniga, C., Wozniak, J. M., Gonzalez, D. J., & Zengler, K. (2018). Optimization of carbon and energy utilization through differential translational efficiency. *Nature Communications*, *9*(1), 4474. https://doi.org/10.1038/s41467-018-06993-6

Azam, F., Fenchel, T., Field, J. G., Gray, J. S., Meyer-Reil, L. A., & Thingstad, F. (1983). The Ecological Role of Water-Column Microbes in the Sea. *Marine Ecology Progress Series*, *10*(3), 257–263. JSTOR.

Berberich, R., Kaback, M., & Freese, E. (1968). D-amino acids as inducers of L-alanine dehydrogenase in Bacillus subtilis. *Journal of Biological Chemistry*, *243*(5), 1006–1011.

Blackburn, N., Fenchel, T., & Mitchell, J. (1998). Microscale Nutrient Patches in Planktonic Habitats Shown by Chemotactic Bacteria. *Science*, *282*(5397), 2254–2256. https://doi.org/10.1126/science.282.5397.2254

Bowen, J. D., Stolzenbach, K. D., & Chisholm, S. W. (1993). Simulating bacterial clustering around phytoplankton cells in a turbulent ocean. *Limnology and Oceanography*, *38*(1), 36–51. https://doi.org/10.4319/lo.1993.38.1.0036

Brumley, D. R., Carrara, F., Hein, A. M., Yawata, Y., Levin, S. A., & Stocker, R. (2019). Bacteria push the limits of chemotactic precision to navigate dynamic chemical gradients. *Proceedings of the National Academy of Sciences*, *116*(22), 10792–10797. https://doi.org/10.1073/pnas.1816621116

Button, D. K. (2004). Life in Extremely Dilute Environments: The Major Role of Oligobacteria. In Bull (Ed.), *Microbial Diversity and Bioprospecting* (pp. 160–168). American Society of Microbiology. https://doi.org/10.1128/9781555817770.ch16

Camacho, C., Coulouris, G., Avagyan, V., Ma, N., Papadopoulos, J., Bealer, K., & Madden, T. L. (2009). BLAST+: Architecture and applications. *BMC Bioinformatics*, *10*(1), 421. https://doi.org/10.1186/1471-2105-10-421

Carini, P., Campbell, E. O., Morré, J., Sañudo-Wilhelmy, S. A., Thrash, J. C., Bennett, S. E., Temperton, B., Begley, T., & Giovannoni, S. J. (2014). Discovery of a SAR11 growth requirement for thiamin's pyrimidine precursor and its distribution in the Sargasso Sea. *The ISME Journal*, *8*(8), 1727–1738.

Carini, P., Steindler, L., Beszteri, S., & Giovannoni, S. J. (2013). Nutrient requirements for growth of the extreme oligotroph '*Candidatus* Pelagibacter ubique'HTCC1062 on a defined medium. *The ISME Journal*, *7*(3), 592–602.

Carini, P., Van Mooy, B. A. S., Thrash, J. C., White, A., Zhao, Y., Campbell, E. O., Fredricks, H. F., & Giovannoni, S. J. (2015). SAR11 lipid renovation in response to phosphate starvation. *Proceedings of the National Academy of Sciences*, *112*(25), 7767–7772. https://doi.org/10.1073/pnas.1505034112

Chuckran, P. F., Hungate, B. A., Schwartz, E., & Dijkstra, P. (2021). Variation in genomic traits of microbial communities among ecosystems. *FEMS Microbes*, xtab020. https://doi.org/10.1093/femsmc/xtab020

Cottrell, M. T., & Kirchman, D. L. (2016). Transcriptional Control in Marine Copiotrophic and Oligotrophic Bacteria with Streamlined Genomes. *Applied and Environmental Microbiology*, *82*(19), 6010–6018. https://doi.org/10.1128/AEM.01299-16

Dusenbery, D. B. (1997). Minimum size limit for useful locomotion by free-swimming microbes. *Proceedings of the National Academy of Sciences*, *94*(20), 10949–10954. https://doi.org/10.1073/pnas.94.20.10949

Fadeev, E., De Pascale, F., Vezzi, A., Hübner, S., Aharonovich, D., & Sher, D. (2016). Why Close a Bacterial Genome? The Plasmid of Alteromonas Macleodii HOT1A3 is a Vector for Inter-Specific Transfer of a Flexible Genomic Island. *Frontiers in Microbiology*, *7*. https://doi.org/10.3389/fmicb.2016.00248

Freese, E., & Oosterwyk, J. (1963). The Induction of Alanine Dehydrogenase. *Biochemistry*, *2*(6), 1212–1216.

Galperin, M. Y., Wolf, Y. I., Makarova, K. S., Vera Alvarez, R., Landsman, D., & Koonin, E. V. (2021). COG database update: Focus on microbial diversity, model organisms, and widespread pathogens. *Nucleic Acids Research*, *49*(D1), D274–D281. https://doi.org/10.1093/nar/gkaa1018

Giovannoni, S. J. (2005). Genome Streamlining in a Cosmopolitan Oceanic Bacterium. *Science*, *309*(5738), 1242–1245. https://doi.org/10.1126/science.1114057

Giovannoni, S. J. (2017). SAR11 Bacteria: The Most Abundant Plankton in the Oceans. *Annual Review of Marine Science*, *9*(1), 231–255. https://doi.org/10.1146/annurev-marine-010814-015934

Giovannoni, S. J., Cameron Thrash, J., & Temperton, B. (2014). Implications of streamlining theory for microbial ecology. *The ISME Journal*, *8*(8), 1553–1565. https://doi.org/10.1038/ismej.2014.60

Giovannoni, S. J., Halsey, K. H., Saw, J., Muslin, O., Suffridge, C. P., Sun, J., Lee, C.-P., Moore, E. R., Temperton, B., & Noell, S. E. (2019). A Parasitic Arsenic Cycle That Shuttles Energy from Phytoplankton to Heterotrophic Bacterioplankton. *MBio*, *10*(2). https://doi.org/10.1128/mBio.00246-19

Graham, E. D., & Tully, B. J. (2021). Marine Dadabacteria exhibit genome streamlining and phototrophy-driven niche partitioning. *The ISME Journal*, *15*(4), 1248–1256. https://doi.org/10.1038/s41396-020-00834-5

Halsey, K. H., Carter, A. E., & Giovannoni, S. J. (2012). Synergistic metabolism of a broad range of C1 compounds in the marine methylotrophic bacterium HTCC2181: C1 metabolism in the marine isolate HTCC2181. *Environmental Microbiology*, *14*(3), 630–640. https://doi.org/10.1111/j.1462-2920.2011.02605.x

Hansell, D. A., Carlson, C. A., Repeta, D. J., & Schlitzer, R. (2009). Dissolved Organic Matter In the Ocean: A Controversy Stimulates New Insights. *Oceanography*, *22*(4), 202–211.

Held, N. A., McIlvin, M. R., Moran, D. M., Laub, M. T., & Saito, M. A. (2019). Unique Patterns and Biogeochemical Relevance of Two-Component Sensing in Marine Bacteria. *MSystems*, *4*(1). https://doi.org/10.1128/mSystems.00317-18

Hellweger, F. L., & Bucci, V. (2009). A bunch of tiny individuals—Individual-based modeling for microbes. *Ecological Modelling*, *220*(1), 8–22. https://doi.org/10.1016/j.ecolmodel.2008.09.004

Hulburt, E. M. (1970). Competition for Nutrients by Marine Phytoplankton in Oceanic, Castal, and Estuarine Regions. *Ecology*, *51*(3), 475–484. https://doi.org/10.2307/1935382

Ivars-Martinez, E., Martin-Cuadrado, A.-B., D'Auria, G., Mira, A., Ferriera, S., Johnson, J., Friedman, R., & Rodriguez-Valera, F. (2008). Comparative genomics of two ecotypes of the marine planktonic copiotroph Alteromonas macleodii suggests alternative lifestyles associated with different kinds of particulate organic matter. *The ISME Journal*, *2*(12), 1194–1212. https://doi.org/10.1038/ismej.2008.74

Jackson, G. A. (1987). Simulating chemosensory responses of marine microorganisms1: Bacterial chemokinesis. *Limnology and Oceanography*, *32*(6), 1253–1266. https://doi.org/10.4319/lo.1987.32.6.1253

Jeong, J.-A., Hyun, J., & Oh, J.-I. (2015). Regulation Mechanism of the *ald* Gene Encoding Alanine Dehydrogenase in Mycobacterium smegmatis and Mycobacterium tuberculosis by the Lrp/AsnC Family Regulator AldR. *Journal of Bacteriology*, *197*(19), 3142–3153. https://doi.org/10.1128/JB.00453-15

Kepes, A. (1963). Kinetic of induced enzyme synthesis determination of the mean life of galactosidase-specific messenger RNA. *Biochimica et Biophysica Acta (BBA) - Specialized Section on Nucleic Acids and Related Subjects*, *76*, 293–309. https://doi.org/10.1016/0926-6550(63)90043-4

Koch, A. L. (1971). The Adaptive Responses of Escherichia coli to a Feast and Famine Existence. In *Advances in Microbial Physiology* (Vol. 6, pp. 147–217). Elsevier. https://doi.org/10.1016/S0065-2911(08)60069-7

Kostadinov, T. S., Siegel, D. A., & Maritorena, S. (2009). Retrieval of the particle size distribution from satellite ocean color observations. *Journal of Geophysical Research*, *114*(C9), C09015. https://doi.org/10.1029/2009JC005303

Lambert, B. S., Fernandez, V. I., & Stocker, R. (2019). Motility drives bacterial encounter with particles responsible for carbon export throughout the ocean. *Limnology and Oceanography Letters*, *4*(5), 113–118. https://doi.org/10.1002/lol2.10113

Lambrecht, S. J., Steglich, C., & Hess, W. R. (2020). A minimum set of regulators to thrive in the ocean. *FEMS Microbiology Reviews*. https://doi.org/10.1093/femsre/fuaa005

Lankiewicz, T. S., Cottrell, M. T., & Kirchman, D. L. (2016). Growth rates and rRNA content of four marine bacteria in pure cultures and in the Delaware estuary. *The ISME Journal*, *10*(4), 823–832. https://doi.org/10.1038/ismej.2015.156

Lauro, F. M., McDougald, D., Thomas, T., Williams, T. J., Egan, S., Rice, S., DeMaere, M. Z., Ting, L., Ertan, H., Johnson, J., Ferriera, S., Lapidus, A., Anderson, I., Kyrpides, N., Munk, A. C., Detter, C., Han, C. S., Brown, M. V., Robb, F. T., … Cavicchioli, R. (2009). The genomic basis of trophic strategy in marine bacteria. *Proceedings of the National Academy of Sciences*, *106*(37), 15527–15533. https://doi.org/10.1073/pnas.0903507106

Lee, C., & Bada, J. L. (1977). Dissolved amino acids in the equatorial Pacific, the Sargasso Sea, and Biscayne Bay1: Seawater dissolved amino acids. *Limnology and Oceanography*, *22*(3), 502–510. https://doi.org/10.4319/lo.1977.22.3.0502

Liang, W., Malhotra, A., & Deutscher, M. P. (2011). Acetylation Regulates the Stability of a Bacterial Protein: Growth Stage-Dependent Modification of RNase R. *Molecular Cell*, *44*(1), 160–166. https://doi.org/10.1016/j.molcel.2011.06.037

Lu, S., Wang, J., Chitsaz, F., Derbyshire, M. K., Geer, R. C., Gonzales, N. R., Gwadz, M., Hurwitz, D. I., Marchler, G. H., Song, J. S., Thanki, N., Yamashita, R. A., Yang, M., Zhang, D., Zheng, C., Lanczycki, C. J., & Marchler-Bauer, A. (2020). CDD/SPARCLE: The conserved domain database in 2020. *Nucleic Acids Research*, *48*(D1), D265–D268. https://doi.org/10.1093/nar/gkz991

Lu, X., Zou, L., Clevinger, C., Liu, Q., Hollibaugh, J. T., & Mou, X. (2014). Temporal dynamics and depth variations of dissolved free amino acids and polyamines in coastal seawater determined by high-performance liquid chromatography. *Marine Chemistry*, *163*, 36–44. https://doi.org/10.1016/j.marchem.2014.04.004

Luchsinger, R. H., Bergersen, B., & Mitchell, J. G. (1999). Bacterial Swimming Strategies and Turbulence. *Biophysical Journal*, *77*(5), 2377–2386. https://doi.org/10.1016/S0006-3495(99)77075-X

Macek, B., Forchhammer, K., Hardouin, J., Weber-Ban, E., Grangeasse, C., & Mijakovic, I. (2019). Protein post-translational modifications in bacteria. *Nature Reviews Microbiology*, *17*(11), 651–664. https://doi.org/10.1038/s41579-019-0243-0

Maier, T., Schmidt, A., Güell, M., Kühner, S., Gavin, A.-C., Aebersold, R., & Serrano, L. (2011). Quantification of mRNA and protein and integration with protein turnover in a bacterium. *Molecular Systems Biology*, *7*, 511. https://doi.org/10.1038/msb.2011.38

McCowen, S. M., & Phibbs, P. V. (1974). Regulation of Alanine Dehydrogenase in Bacillus licheniformis. *Journal of Bacteriology*, *118*(2), 590.

Meyer, M. M., Ames, T. D., Smith, D. P., Weinberg, Z., Schwalbach, M. S., Giovannoni, S. J., & Breaker, R. R. (2009). Identification of candidate structured RNAs in the marine organism "Candidatus Pelagibacter ubique." *BMC Genomics*, *10*(1), 268. https://doi.org/10.1186/1471-2164-10-268

Mitchell, J. G. (1991). The influence of cell size on marine bacterial motility and energetics. *Microbial Ecology*, *22*(1), 227–238. https://doi.org/10.1007/BF02540225

Mopper, K., & Lindroth, P. (1982). Diel and depth variations in dissolved free amino acids and ammonium in the Baltic Sea determined by shipboard HPLC analysis1: Shipboard amino acid analyses. *Limnology and Oceanography*, *27*(2), 336–347. https://doi.org/10.4319/lo.1982.27.2.0336

Moriarty, D. J. W., & Bell, R. T. (1993). Bacterial Growth and Starvation in Aquatic Environments. In S. Kjelleberg (Ed.), *Starvation in Bacteria* (pp. 25–53). Springer US. https://doi.org/10.1007/978-1-4899-2439-1_2

Morita, R. Y. (1982). Starvation-Survival of Heterotrophs in the Marine Environment. In K. C. Marshall (Ed.), *Advances in Microbial Ecology* (Vol. 6, pp. 171–198). Springer US. https://doi.org/10.1007/978-1-4615-8318-9_5

Morris, R. M., Rappé, M. S., Connon, S. A., Vergin, K. L., Siebold, W. A., Carlson, C. A., & Giovannoni, S. J. (2002). SAR11 clade dominates ocean surface bacterioplankton communities. *Nature*, *420*(6917), 806–810. https://doi.org/10.1038/nature01240

Noell, S. E., Barrell, G. E., Suffridge, C., Morré, J., Gable, K. P., Graff, J. R., VerWey, B. J., Hellweger, F. L., & Giovannoni, S. J. (2021). SAR11 Cells Rely on Enzyme Multifunctionality To Metabolize a Range of Polyamine Compounds. *MBio*, 2021.05.13.444117. https://doi.org/10.1128/mBio.01091-21

Noell, S. E., & Giovannoni, S. J. (2019). SAR11 bacteria have a high affinity and multifunctional glycine betaine transporter. *Environmental Microbiology*, *21*(7), 2559–2575. https://doi.org/10.1111/1462-2920.14649

Ottesen, E. A., Young, C. R., Gifford, S. M., Eppley, J. M., Marin, R., Schuster, S. C., Scholin, C. A., & DeLong, E. F. (2014). Multispecies diel transcriptional oscillations in open ocean heterotrophic bacterial assemblages. *Science*, *345*(6193), 207–212. https://doi.org/10.1126/science.1252476

Pardee, A. B., & Prestidge, L. S. (1961). The initial kinetics of enzyme induction. *Biochimica et Biophysica Acta*, *49*(1), 77–88. https://doi.org/10.1016/0006-3002(61)90871-X

Pilskaln, C. H., Villareal, T. A., Dennett, M., Darkangelo-Wood, C., & Meadows, G. (2005). High concentrations of marine snow and diatom algal mats in the North Pacific Subtropical Gyre: Implications

for carbon and nitrogen cycles in the oligotrophic ocean. *Deep Sea Research Part I: Oceanographic Research Papers*, *52*(12), 2315–2332. https://doi.org/10.1016/j.dsr.2005.08.004

Pocklington, R. (1971). Physical Sciences: Free Amino-acids dissolved in North Atlantic Ocean Waters. *Nature*, *230*(5293), 374–375. https://doi.org/10.1038/230374a0

Poindexter, J. S. (1981). Oligotrophy. In M. Alexander (Ed.), *Advances in Microbial Ecology* (pp. 63–89). Springer US. https://doi.org/10.1007/978-1-4615-8306-6_2

Porumb, H., Vancea, D., Mureşan, L., Presecan, E., Lascu, I., Petrescu, I., Porumb, T., Pop, R., & Bârzu, O. (1987). Structural and catalytic properties of L-alanine dehydrogenase from Bacillus cereus. *The Journal of Biological Chemistry*, *262*(10), 4610–4615.

R Core Team, -. (n.d.). *R: A language and environment for statistical computing*. https://www.R-project.org/

Scanlan, D. J., Ostrowski, M., Mazard, S., Dufresne, A., Garczarek, L., Hess, W. R., Post, A. F., Hagemann, M., Paulsen, I., & Partensky, F. (2009). Ecological Genomics of Marine Picocyanobacteria. *Microbiology and Molecular Biology Reviews*, *73*(2), 249–299. https://doi.org/10.1128/MMBR.00035-08

Schuster, M. (2011). Global Expression Analysis of Quorum-Sensing Controlled Genes. In K. P. Rumbaugh (Ed.), *Quorum Sensing* (Vol. 692, pp. 173–187). Humana Press. https://doi.org/10.1007/978-1-60761-971-0_13

Schwengers, O., Jelonek, L., Dieckmann, M. A., Beyvers, S., Blom, J., & Goesmann, A. (2021). Bakta: Rapid and standardized annotation of bacterial genomes via alignment-free sequence identification. *Microbial Genomics*, *7*(11). https://doi.org/10.1099/mgen.0.000685

Seymour, J. R., Marcos, & Stocker, R. (2009). Resource Patch Formation and Exploitation throughout the Marine Microbial Food Web. *The American Naturalist*, *173*(1), E15–E29. https://doi.org/10.1086/593004

Sher, D., Thompson, J. W., Kashtan, N., Croal, L., & Chisholm, S. W. (2011). Response of Prochlorococcus ecotypes to co-culture with diverse marine bacteria. *The ISME Journal*, *5*(7), 1125–1132. https://doi.org/10.1038/ismej.2011.1

Siegel, D. A. (1998). Resource competition in a discrete environment: Why are plankton distributions paradoxical? *Limnology and Oceanography*, *43*(6), 1133–1146. https://doi.org/10.4319/lo.1998.43.6.1133

Siranosian, K. J., Ireton, K., & Grossman, A. D. (1993). Alanine dehydrogenase (ald) is required for normal sporulation in Bacillus subtilis. *Journal of Bacteriology*, *175*(21), 6789–6796. https://doi.org/10.1128/JB.175.21.6789-6796.1993

Smith, D. P., Kitner, J. B., Norbeck, A. D., Clauss, T. R., Lipton, M. S., Schwalbach, M. S., Steindler, L., Nicora, C. D., Smith, R. D., & Giovannoni, S. J. (2010). Transcriptional and Translational Regulatory Responses to Iron Limitation in the Globally Distributed Marine Bacterium Candidatus Pelagibacter ubique. *PLoS ONE*, *5*(5), e10487. https://doi.org/10.1371/journal.pone.0010487

Smith, D. P., Nicora, C. D., Carini, P., Lipton, M. S., Norbeck, A. D., Smith, R. D., & Giovannoni, S. J. (2016). Proteome Remodeling in Response to Sulfur Limitation in " *Candidatus* Pelagibacter ubique." *MSystems*, *1*(4), e00068-16. https://doi.org/10.1128/mSystems.00068-16

Smith, D. P., Thrash, J. C., Nicora, C. D., Lipton, M. S., Burnum-Johnson, K. E., Carini, P., Smith, R. D., & Giovannoni, S. J. (2013). Proteomic and Transcriptomic Analyses of "*Candidatus* Pelagibacter ubique"

Describe the First PII-Independent Response to Nitrogen Limitation in a Free-Living Alphaproteobacterium. *MBio*, *4*(6), e00133-12-e00133-12. https://doi.org/10.1128/mBio.00133-12

Son, K., Menolascina, F., & Stocker, R. (2016). Speed-dependent chemotactic precision in marine bacteria. *Proceedings of the National Academy of Sciences of the United States of America*, *113*(31), 8624–8629. https://doi.org/10.1073/pnas.1602307113

Sowell, S. M., Norbeck, A. D., Lipton, M. S., Nicora, C. D., Callister, S. J., Smith, R. D., Barofsky, D. F., & Giovannoni, S. J. (2008). Proteomic Analysis of Stationary Phase in the Marine Bacterium "Candidatus Pelagibacter ubique." *Applied and Environmental Microbiology*, *74*(13), 4091–4100. https://doi.org/10.1128/AEM.00599-08

Steindler, L., Schwalbach, M. S., Smith, D. P., Chan, F., & Giovannoni, S. J. (2011). Energy Starved Candidatus Pelagibacter Ubique Substitutes Light-Mediated ATP Production for Endogenous Carbon Respiration. *PLoS ONE*, *6*(5), e19725. https://doi.org/10.1371/journal.pone.0019725

Stingl, U., Tripp, H. J., & Giovannoni, S. J. (2007). Improvements of high-throughput culturing yielded novel SAR11 strains and other abundant marine bacteria from the Oregon coast and the Bermuda Atlantic Time Series study site. *The ISME Journal*, *1*(4), 361–371. https://doi.org/10.1038/ismej.2007.49

Stocker, R. (2012). Marine Microbes See a Sea of Gradients. *Science*, *338*(6107), 628–633. https://doi.org/10.1126/science.1208929

Stocker, R., Seymour, J. R., Samadani, A., Hunt, D. E., & Polz, M. F. (2008). Rapid chemotactic response enables marine bacteria to exploit ephemeral microscale nutrient patches. *Proceedings of the National Academy of Sciences*, *105*(11), 4209–4214. https://doi.org/10.1073/pnas.0709765105

Striebel, F., Imkamp, F., Özcelik, D., & Weber-Ban, E. (2014). Pupylation as a signal for proteasomal degradation in bacteria. *Biochimica et Biophysica Acta (BBA) - Molecular Cell Research*, *1843*(1), 103–113. https://doi.org/10.1016/j.bbamcr.2013.03.022

Sun, J., Todd, J. D., Thrash, J. C., Qian, Y., Qian, M. C., Temperton, B., Guo, J., Fowler, E. K., Aldrich, J. T., Nicora, C. D., Lipton, M. S., Smith, R. D., De Leenheer, P., Payne, S. H., Johnston, A. W. B., Davie-Martin, C. L., Halsey, K. H., & Giovannoni, S. J. (2016). The abundant marine bacterium *Pelagibacter* simultaneously catabolizes dimethylsulfoniopropionate to the gases dimethyl sulfide and methanethiol. *Nature Microbiology*, *1*(8), 16065. https://doi.org/10.1038/nmicrobiol.2016.65

Taylor, J. R., & Stocker, R. (2012). Trade-Offs of Chemotactic Foraging in Turbulent Water. *Science*, *338*(6107), 675–679. https://doi.org/10.1126/science.1219417

Taylor, R. C., Webb Robertson, B.-J. M., Markillie, L. M., Serres, M. H., Linggi, B. E., Aldrich, J. T., Hill, E. A., Romine, M. F., Lipton, M. S., & Wiley, H. S. (2013). Changes in translational efficiency is a dominant regulatory mechanism in the environmental response of bacteria. *Integrative Biology*, *5*(11), 1393. https://doi.org/10.1039/c3ib40120k

Tripp, H. J., Schwalbach, M. S., Meyer, M. M., Kitner, J. B., Breaker, R. R., & Giovannoni, S. J. (2009). Unique glycine-activated riboswitch linked to glycine-serine auxotrophy in SAR11. *Environmental Microbiology*, *11*(1), 230–238. https://doi.org/10.1111/j.1462-2920.2008.01758.x

Tully, B. J., Graham, E. D., & Heidelberg, J. F. (2018). The reconstruction of 2,631 draft metagenome-assembled genomes from the global oceans. *Scientific Data*, *5*(1), 170203. https://doi.org/10.1038/sdata.2017.203

Vandesompele, J., De Preter, K., Pattyn, F., Poppe, B., Van Roy, N., De Paepe, A., & Speleman, F. (2002). Accurate normalization of real-time quantitative RT-PCR data by geometric averaging of multiple internal control genes. *Genome Biology*, *3*(7), RESEARCH0034. https://doi.org/10.1186/gb-2002-3-7-research0034

Weissman, J. L., Hou, S., & Fuhrman, J. A. (2021). Estimating maximal microbial growth rates from cultures, metagenomes, and single cells via codon usage patterns. *Proceedings of the National Academy of Sciences*, *118*(12), e2016810118. https://doi.org/10.1073/pnas.2016810118

Wickham, H. (2016). *ggplot2: Elegant Graphics for Data Analysis*. Springer-Verlag.

Yawata, Y., Carrara, F., Menolascina, F., & Stocker, R. (2020). Constrained optimal foraging by marine bacterioplankton on particulate organic matter. *Proceedings of the National Academy of Sciences*, *117*(41), 25571–25579. https://doi.org/10.1073/pnas.2012443117

Figures

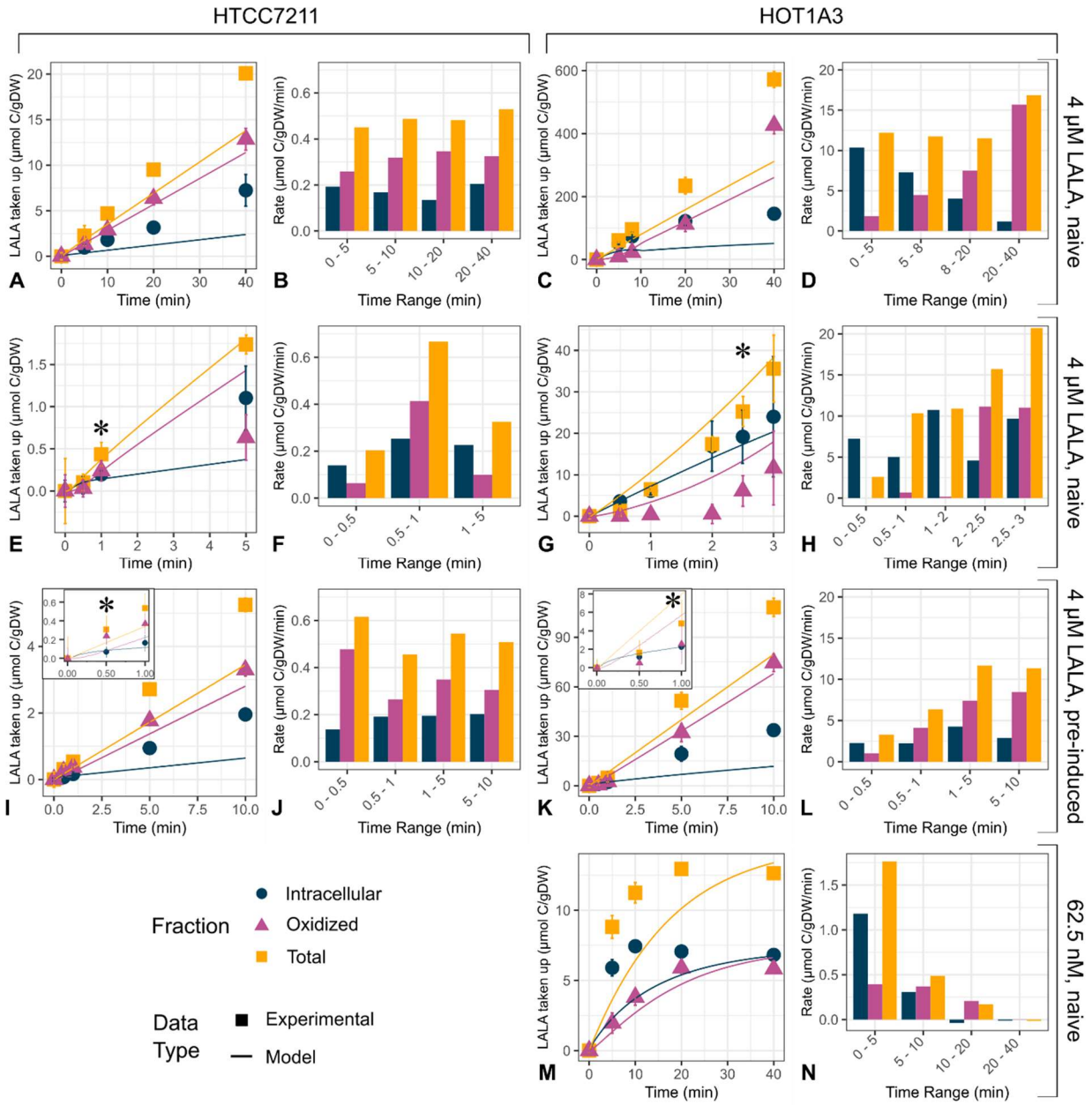

854

855 Figure 1 Uptake and oxidation of [^{14}C]L-alanine ([^{14}C]LALA) in (A-B, E-F, I-J) an oligotroph,

856 *Ca. P.* st. HTCC7211, and (C-D, G-H, K-N) a copiotroph, *A. macleodii* st. HOT1A3, to

857 determine induction and time to initiation of uptake and oxidation. (A, C, E, G, I, K, M) Time

858 course of uptake and oxidation of [^{14}C]LALA in both strains. Points are experimental data, while

859 the lines are the output of the mechanistic model. (B, D, F, H, J, L, N) Bar plots of calculated

860 [^{14}C]LALA uptake, oxidation, and intracellular accumulation rates in the indicated time intervals

861 based on data presented in time course plots. Cells were grown either without (A-H, M-N) or
862 with (I-L) 4 μM LALA prior to harvesting, washing, and starving. Cells were then incubated
863 with either 4 μM (A-L) or 62.5 nM (M-N) of [^{14}C]LALA. (A-D) To determine presence of
864 induction, time points out to 40 min were taken. (E-H) To determine the time until oxidation
865 initiation, short time points were used. (I-L) The experiment was repeated to 10 min with cells
866 that were pre-exposed to LALA for 2 generations before cells were harvested. For detailed
867 explanation of the different fractions, see Methods. Error bars on points are the standard
868 deviation of triplicate cultures. Where there are error bars, they are too small to be visible. *
869 indicates oxidation initiation, the first time point where oxidation was greater than zero and the
870 standard deviation did not overlap zero. Note that y- and x-axis scales differ between plots.

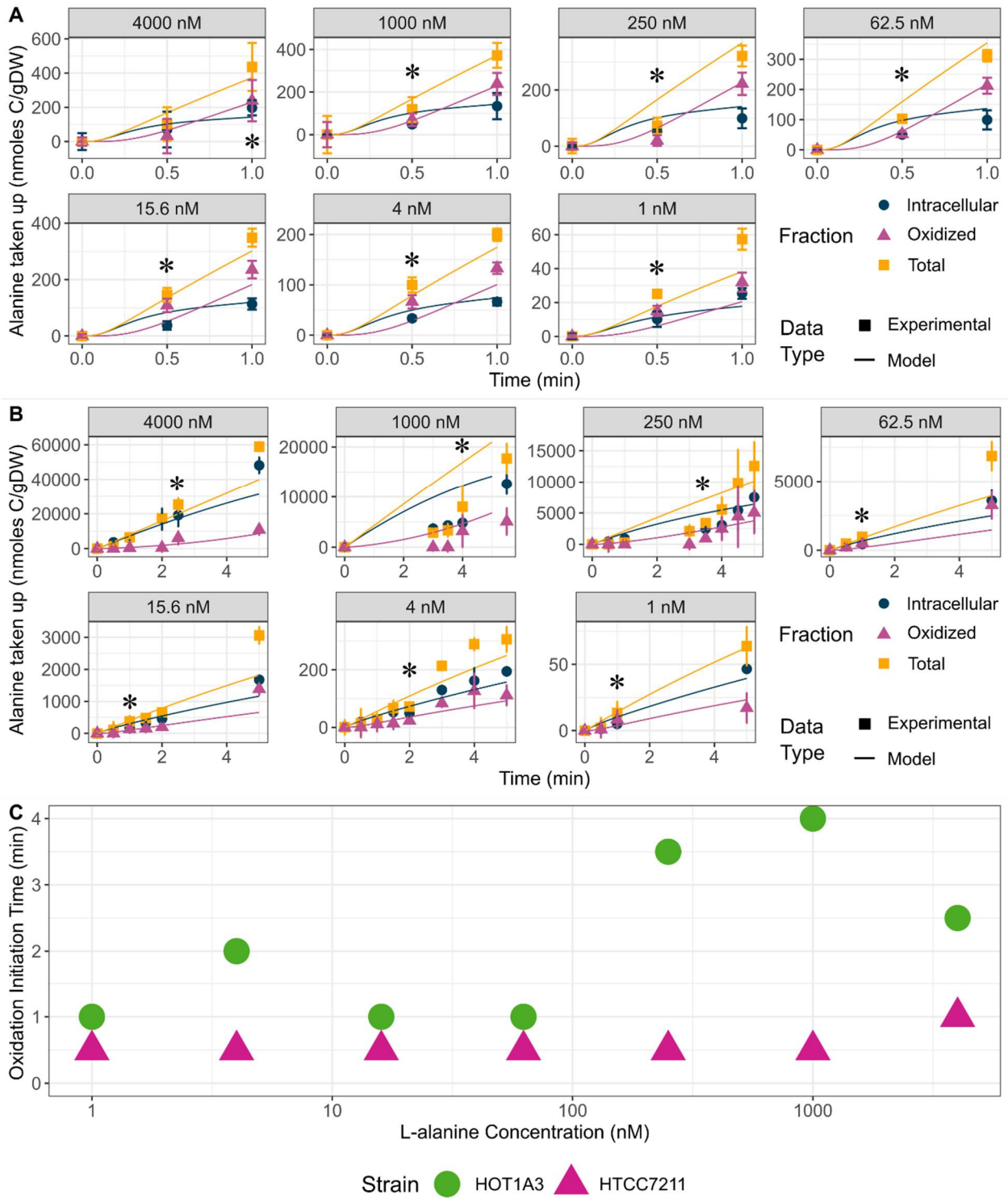

871

872 Figure 2 Uptake and oxidation of [^{14}C]L-alanine ([^{14}C]LALA) in (A) an oligotroph, *Ca. P.* st.

873 HTCC7211, and (B) a copiotroph, *A. macleodii* st. HOT1A3, to determine initiation of oxidation

874 at various concentrations. Points are experimental data, while lines are the output of a
875 mechanistic model of intracellular LALA accumulation and metabolism in these strains. Cells
876 used were naïve to LALA prior to harvesting, washing, and starving. For detailed explanation of
877 the different fractions, see Methods. Error bars on the points are the standard deviation of
878 triplicate cultures. * indicates oxidation initiation, the first time point where oxidation was
879 greater than zero and the standard deviation did not overlap zero. Note that the y- and x-axis
880 scales differ between plots. (C) Plot showing times of initiation of LALA oxidation in the two
881 strains over the range of measured LALA concentrations, based on data presented in (A) and (B).
882 The x-axis is in a $\log_{10}$ scale to allow differentiation of concentrations.
883

884

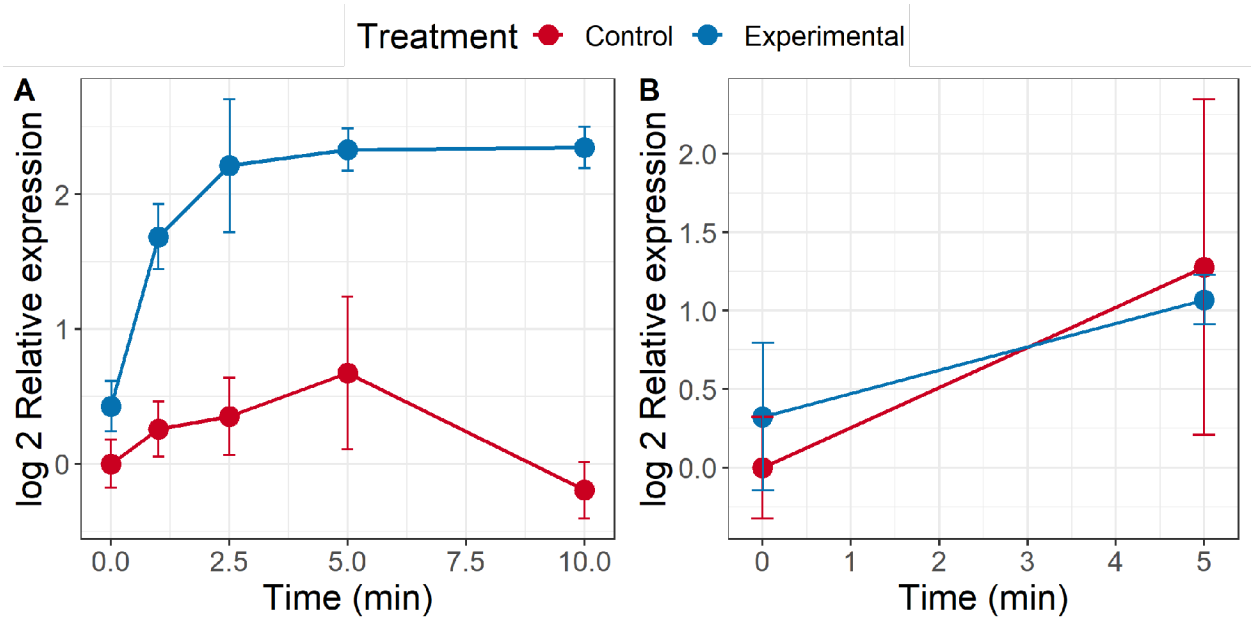

885

886 Figure 3 Results from a reverse transcription quantitative real-time PCR (RT-qPCR) experiment
887 measuring transcripts for the alanine dehydrogenase gene in (A) *A. macleodii* st. HOT1A3 or (B)
888 *Cand.* P. st. HTCC7211. Experimental cultures in both had 4 µM LALA added; an equal volume
889 of water was added to the control cultures. *ALD* transcript abundances were normalized to the
890 abundances of two endogenous control genes, *recA* and *rpoD*. Final abundances were further
891 normalized to the average of the control time zero abundances. Error bars are the standard
892 deviation of four replicates: in HOT1A3, duplicate biological replicates were each split into
893 duplicate technical replicates; in HTCC7211, quadruplicate biological replicates were used for
894 each time point.

895

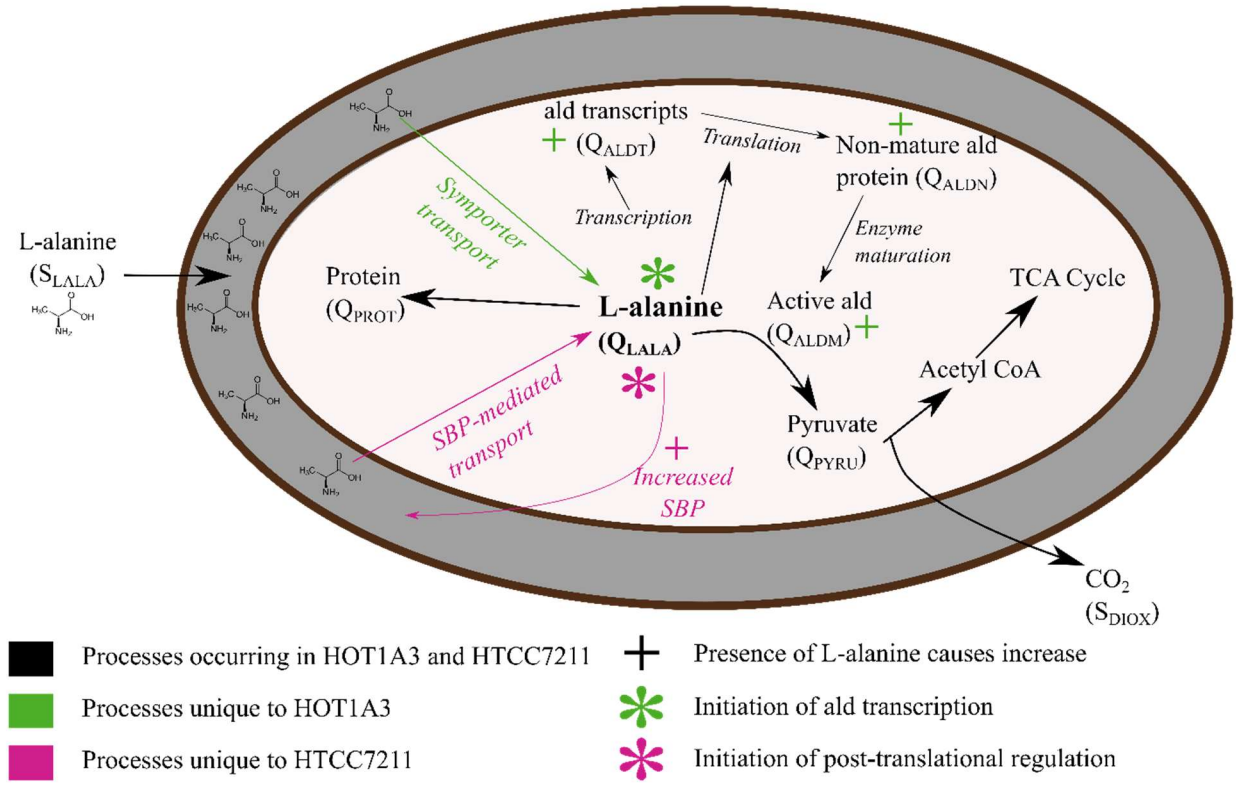

Figure 4 Depiction of proposed model for uptake and metabolism of L-alanine in either a copiotroph, *Alteromonas macleodii* st. HOT1A3 (green) or an oligotroph, *Ca. P.* st. HTCC7211 (pink). Transcription, translation, and enzyme maturation of alanine dehydrogenase gene (*ald*) happen constantly in HTCC7211. SBP: substrate-binding protein. For a full explanation of the model and rationale, see the text.

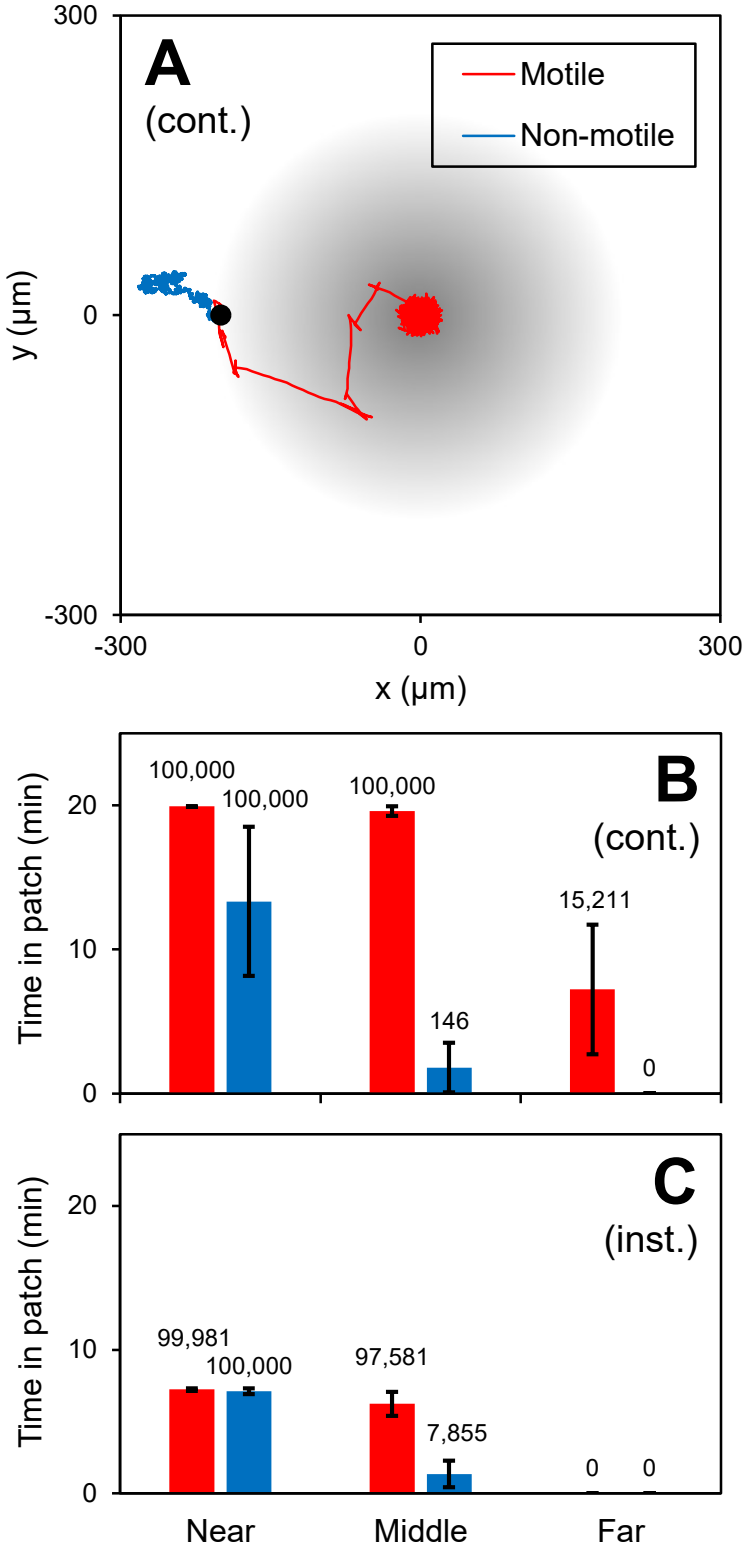
A
(cont.)
Motile
Non-motile
300
0
-300
y (µm)
-300
0
300
x (µm)
B
(cont.)
Time in patch (min)
20
10
0
100,000
100,000
100,000
146
15,211
0
C
(inst.)
Time in patch (min)
20
10
0
99,981
100,000
97,581
7,855
0
0
Near
Middle
Far

904

Figure 5 Exposure time of motile and non-motile cells to a continuous source (i.e., leaking phytoplankton cell) and an instantaneous source (i.e., lysing phytoplankton cell) of nutrients. (A) Example of cell trajectories for the continuous source scenario. Cells were initially placed 200 µm from the source (black symbol; Middle scenario). (B-C) Average time spent in patch for those cells that enter it. Cells were initially placed at 20 µm ("Near"), 200 µm ("Middle") and 2,000 µm ("Far") from the source. Labels indicate number of cells out of 100,000 that reach the patch. Simulations were run for 20 min., which constitutes an upper bound on the patch residence times. Error bars are standard deviation.